PNAS RESEARCH ARTICLE | EVOLUTION

Biomechanics of the mandibular middle ear of the cynodont *Thrinaxodon* and the evolution of mammal hearing

Alec T. Wilken[a,1], Chelsie C. G. Snipes[a], Callum F. Ross[a], and Zhe-Xi Luo[a,1]

Affiliations are included on p. 10.

Edited by Geerat Vermeij, University of California, Davis, CA; received June 18, 2025; accepted October 31, 2025

The middle ear of mammals is a major functional innovation, distinctive in that it is detached from the mandible and has a tympanic membrane supported by a ring-like ectotympanic. These novelties of the middle ear have enabled modern mammals to develop more sensitive hearing than all other tetrapods, especially at higher frequencies. Fossils from recent decades have clarified the evolution of the detached middle ear from the jaw bones of Paleozoic therapsids and Mesozoic cynodonts, and the evolution of the tympanum. These discoveries make it possible to answer important questions about the functional significance of these features. Here, we evaluate the relative hearing efficacy of a well-known cynodont precursor to mammals, *Thrinaxodon liorhinus*. Using finite element analysis (FEA), we calculated the harmonic response of the *Thrinaxodon* ear to bone-conducted and airborne sound and estimated the sound pressure level (SPL) at the stapedial footplate across a broad range of frequencies. We provide evidence that airborne sound received at the tympanum was the most effective mode of sound reception in *Thrinaxodon*. In contrast, bone conducted sound through the mandibular bones barely met our estimated hearing threshold. Our findings suggest that, like modern mammals, cynodonts were already reliant on a soft tissue tympanum to receive airborne sound, albeit with limited sensitivity to high frequencies. This is a detailed biomechanical evaluation of tympanum function in the cynodont predecessors of mammals and yields insight into the sequence of functional innovations during the evolution of mammal hearing.

tympanic membrane | finite element modeling | hearing evolution | therapsids | mammals

Significance

The middle ear of modern mammals is detached from the mandible and has a soft-tissue eardrum, which allows airborne sound to be heard across a wide range of frequencies. A rich fossil record shows that the middle ear bones of mammals evolved from the jaw bones of their synapsid predecessors, but how this transformation was associated with changes in hearing function is unknown. Our finite element analysis (FEA) of the harmonic response of the mandibular ear bones and soft-tissue eardrum of the synapsid *Thrinaxodon* suggests that this 250-Mya-old mammal precursor was already capable of tympanic hearing similar to extant mammals and provides evidence that this functional transition occurred very early in mammal evolutionary history.

The highly derived middle and inner ears of mammals enable their enhanced hearing capabilities relative to other tetrapods, particularly through increased sensitivity to a broader and higher frequency range (1–3). This hallmark adaptation enabled early mammals to occupy nocturnal niches in the Mesozoic (4, 5), and to radiate into a wide range of auditory niches in the Cenozoic, including high frequency echolocation in bats and toothed whales, seismic hearing in blind mole rats and golden moles, and long-distance infrasonic hearing in elephants and baleen whales (6, 7). This extraordinary diversity of hearing function is a manifest feature of the adaptive radiation of mammals (6, 7).

The evolution of the mammalian middle ear is the most thoroughly documented morphological transformation in mammalian evolutionary history and exemplifies a profound case of exaptation (3, 8–11). An abundant fossil record shows that the malleus, incus, and ectotympanic ear bones of living mammals were derived from the postdentary bones of Paleozoic therapsids and Mesozoic cynodonts through their detachment from the mandible, change in shape, and reduction in size (Fig. 1) (3, 8–13) (*SI Appendix*, Text S1). The ectotympanic ultimately provided attachment for a soft tissue ear drum, or tympanum, initially on the surface of the head, then subsequently at the deep end of an external meatal tube. The tympanum and its associated ossicles evolved from the precursor mandibular middle ear of therapsids, which had dual functions as part of the jaw joint during chewing and the auditory apparatus during hearing (8) (Fig. 1).

Allin (8) hypothesized a postdentary origin of the mammalian tympanum, meaning that the modern mammal middle ear tympanum evolved exclusively from a precursor membrane housed in the lateral cleft of the angular bone (ectotympanic) in fossil cynodonts and therocephalian therapsids, without any structural relationship to the postquadrate tympanum in sauropsids. This scenario has been corroborated and further expanded by genetic studies of middle ear morphogenesis in amniotes (14, 15), as well as by new fossil evidence on the postdentary-attached middle ear in cynodonts that are phylogenetically close to mammaliaforms (16–19) and in early-divergent mammaliaform clades, such as *Sinoconodon*, *Morganucodon* and its relatives, and docodonts (20–27). Among the stem therian clades of the crown Mammalia, the Meckelian-attached middle ear is also found in eutriconodonts and spalacotherioids (26–31). Evaluating the morphological

Author contributions: A.T.W., C.F.R., and Z.-X.L. designed research; A.T.W. and Z.-X.L. performed research; C.C.G.S., C.F.R., and Z.-X.L. contributed new reagents/analytic tools; A.T.W. analyzed data; and A.T.W., C.C.G.S., C.F.R., and Z.-X.L. wrote the paper.

The authors declare no competing interest.

This article is a PNAS Direct Submission.

[1]To whom correspondence may be addressed. Email: atwilken@uchicago.edu or zxluo@uchicago.edu.

This article contains supporting information online at https://www.pnas.org/lookup/suppl/doi:10.1073/pnas.2516082122/-/DCSupplemental.

Published December 8, 2025.

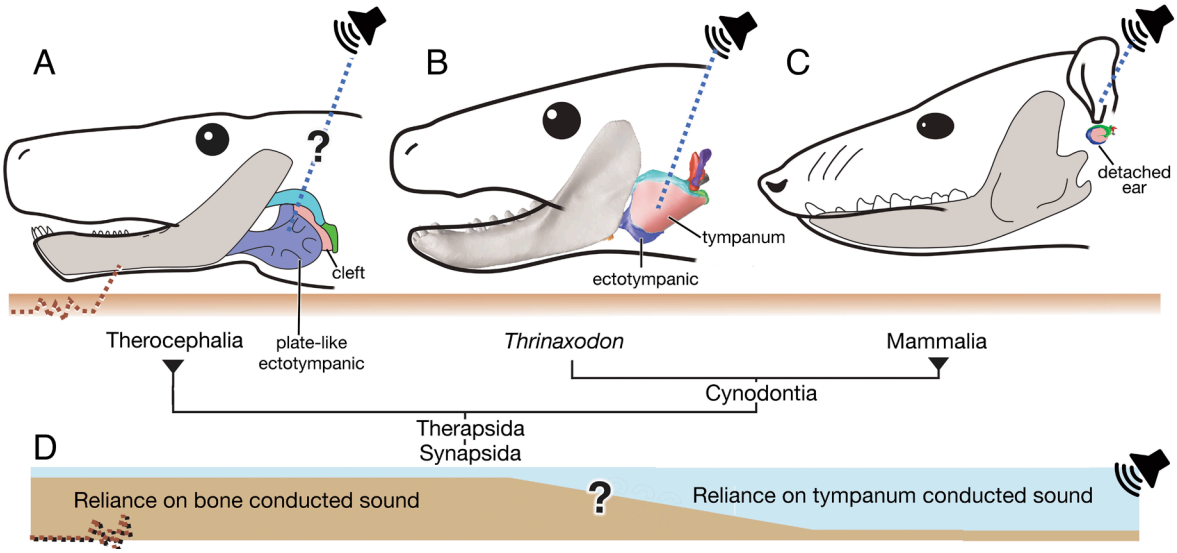

Fig. 1. Evolution of the mandibular middle ear and auditory function. (*A*) In therapsids, the mandibular middle ear included middle ear bones attached to the mandible and a plate-like bony ectotympanic, which is hypothesized to have functioned as a sound receiver. The narrow cleft may have been bridged with a tympanum but hearing likely relied primarily on bone conduction. (*B*) *Thrinaxodon*, the focus of this study, is a cynodont with a mandibular middle ear and a large soft-tissue tympanum for hearing. We hypothesized that the mandibular middle ear of *Thrinaxodon* functioned primarily through airborne sound conduction. (*C*) In the extant mammal *Didelphis,* the middle ear is detached from the mandible, and the soft-tissue tympanum serves as the primary receiver for airborne sound. (*D*) Over synapsid-mammal evolution, auditory function transitioned from reliance on bone-conducted sound in atympanic synapsids to airborne sound detection via a soft-tissue tympanum in modern mammals. Detailed phylogeny in Fig. 5.

transformations of the middle ear in fossil species within a phylogenetic framework has enriched our understanding of the osteological evolution of the mammal ear (3, 24, 26, 29–32) and prompted questions about the significance of these changes for hearing function.

Functional interpretations of the mandibular middle ear of cynodonts, including *Thrinaxodon*, are of particular interest because the middle ear bones were presumably used for both feeding and hearing (Fig. 1) (8, 21, 33–38). The articular (the homolog of the malleus in extant mammals) and the quadrate (the homolog of the incus) still functioned as a load-bearing jaw joint in *Thrinaxodon*, and for that reason were quite large (39). The angular (the homolog of the ectotympanic) and the articular provided attachment for a tympanic membrane which would transmit airborne sound to the articular, through the jaw joint, the quadrate, and to the inner ear via the stapes. Further, it has been hypothesized that the postdentary bones could transmit sound from the rest of the mandible (8) via bone conduction from both the air and the substrate. Many extant tetrapods use bone conduction for hearing. It is likely that some nonmammalian therapsids heard using bone conduction through the cranium and/or the mandibular postdentary bones, including the plate-like reflected lamina of the ectotympanic (Fig. 1*A* and *SI Appendix*, Text S2) (11, 21, 40, 41). What is unclear is how these two alternate routes of sound transmission—airborne and bone conduction—individually and in combination, impacted hearing sensitivity and frequency range in cynodonts, such as *Thrinaxodon*. How did these premammalian cynodonts hear?

A mandibular middle ear with a functional tympanum has long been hypothesized for stem mammals (8, 11, 20, 21, 31, 38, 40–45). However, there is a dearth of direct biomechanical tests of tympanum function in stem mammals. Function of the tympanum with the mandibular middle ear of stem mammalian fossils was interpreted by lever mechanical analyses, including calculation of the middle ear transformer ratio of *Morganucodon* (21, 42) and *Chiniquodon* (43), estimates of the resonance frequency of the ectotympanic in dicynodonts (44), and allometrical analysis of the ectotympanic in therocephalians (45). Previous studies have found that there is a scaling relationship among the middle ear structures involved in sound transmission (41, 42). However, these studies are not fully integrated functional analyses of the mandibular ear system, as they focused only on isolated components of the ear–jaw system and did not account for the stiffness of the ear–jaw interface. To address this deficiency, we present here a finite element model (FEM) of auditory function in the cynodont, *Thrinaxodon* (Fig. 2 and Movie S1). FE analysis (FEA) has proven to be a powerful tool for the study of middle ear function in extant mammals (46–51). Here, we use it to compare the relative hearing efficacy of airborne and bone conduction routes in the early cynodont *Thrinaxodon liorhinus* (Figs. 3 and 4 and *SI Appendix*, Figs. S1–S6). We hypothesized that the direct reception of airborne sound via the tympanic membrane is more effective than sound received via bone conduction through the reflected lamina of the ectotympanic and the mandible (Fig. 1 and Movie S1).

We also used phylogenetic comparative methods to quantify the evolutionary changes in key features of hearing function across the therapsid-mammal lineage, including tympanic membrane area, the primary transformer ratio, and sound pressure gain (Fig. 5 and *SI Appendix*, Fig. S1). This analysis highlights two key anatomical transformations that are most important for therapsid-mammal middle ear hearing evolution and sheds light on the early functional evolution of the mammal middle ear, a defining trait of mammals.

Materials and Methods

Fossil Specimens and CT Scans. The foundation of this study is our anatomical model of the mandible and middle ear of the cynodont *T. liorhinus* (Fig. 2 and Movie S2) from which we obtained measurements of traits involved in hearing function and built a FE model to estimate hearing sensitivity across the hearing range of *Thrinaxodon*. The 3D anatomical model of *Thrinaxodon* was derived from micro-computed tomography (μCT) scans of two specimens: UCMP V40466 (University of California Berkeley Museum of Paleontology) and BP/1/7199 (Evolutionary Studies Institute, Johannesburg, South Africa). Specimen UCMP V40466 was μCT scanned

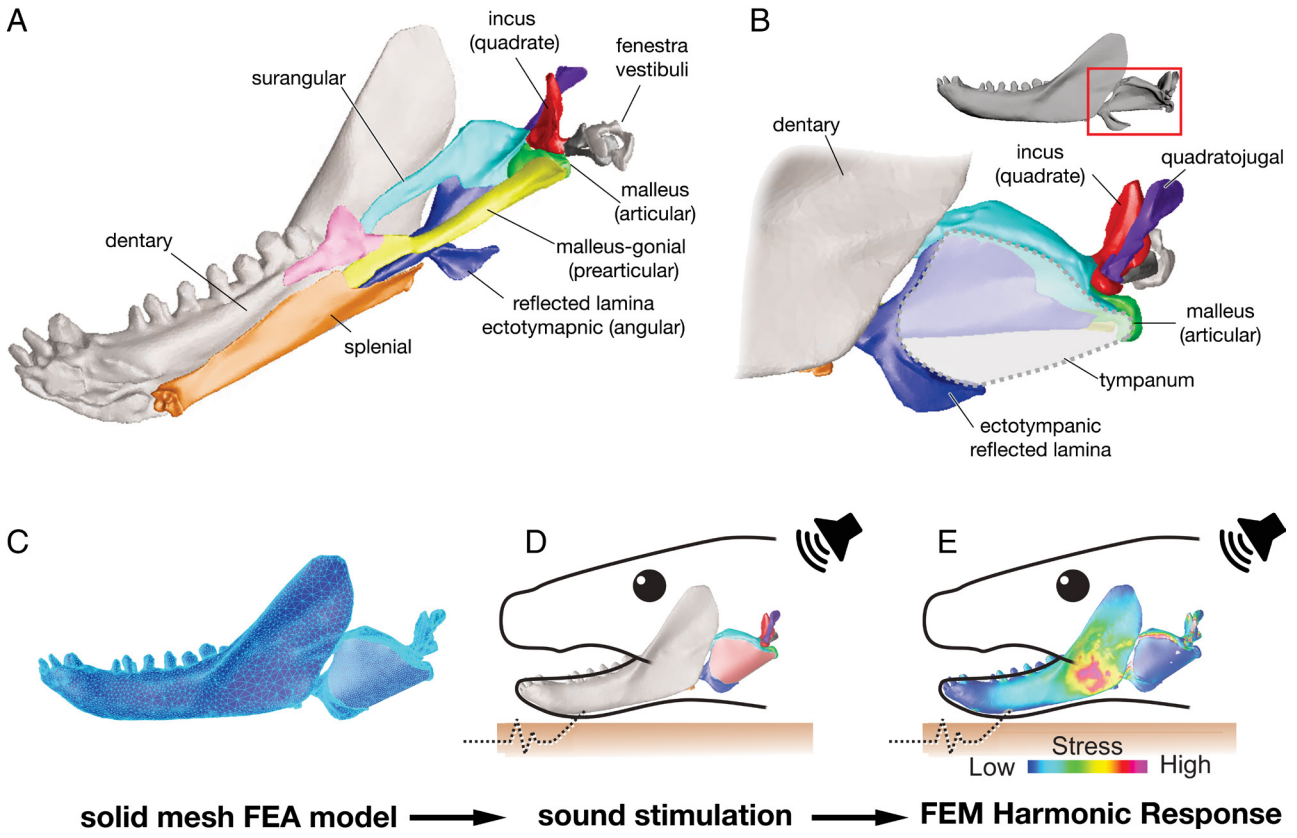

Fig. 2. Structure of the mandibular middle ear of the cynodont *Thrinaxodon* and finite element analysis (FEA) of its hearing biomechanics. (*A*) Mandible and mandibular middle ear (*Right*, oblique medial view; details in Movie S2). (*B*) Mandibular middle ear (*Left*, lateral view). (*C–E*) Finite element modeling of the harmonic response of the mandibular middle ear. (*C*) FEA solid model. (*D*) Simulation of sound pressure level (SPL) on the anatomical model. (*E*) FEM harmonic response in pressure and frequency sensitivity of the mandibular ear, simulated at 1,000 Hz with an input pressure of 58.089 dB. See Movie S1 (URL) for the vibroacoustic response of the mandibular middle ear at 1,000 Hz.

at a voxel size of 39.209 μm at the PaleoCT Laboratory at the University of Chicago. This fossil is largely complete, but the reflected lamina of the ectotympanic is slightly damaged. We reconstructed the reflected lamina using specimen BP/1/7199 from a synchrotron scan by Fernandez et al. (52), accessed through the repository of European Synchrotron Radiation Facility (ERSF) (retrieved in 2023). A specimen of *Didelphis virginiana* (UCRC RV183) from the UChicago Research Collection was μCT scanned at a voxel size of 10.736 μm and modeled to evaluate the utility and the limits of our modeling methods with an extant mammal.

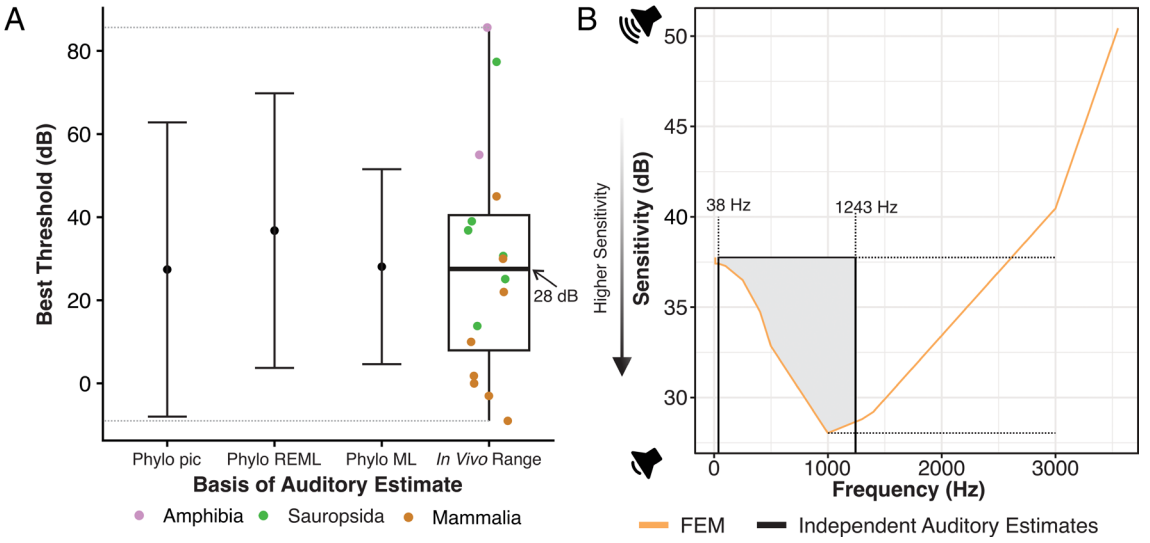

Fig. 3. Calibration of audiometric parameters for the hearing range of *Thrinaxodon*. (*A*) Comparative estimates of the best (lowest) sound pressure threshold by Phylogenetic Comparative Methods: Phylo-pic—Phylogenetic Independent Contrast analysis; Phylo-REML—Phylogenetic Restrictive Maximum Likelihood Analysis; Phylo-ML—Phylogenetic Maximum Likelihood Analysis. Box-Whisker plot of hearing ranges of in vivo observation (best thresholds dB) of tetrapods with known audiograms (*SI Appendix*, Table S1). (*B*) Frequency sensitivity estimates of *Thrinaxodon* ear: Orange line—auditory frequency curve from FEA harmonic response model: *Thrinaxodon* hearing range is from 10 to 2,650 Hz at 38 dB, and its best frequency is 1,000 Hz at minimal 28 dB SPL. The gray area is a more conservative auditory estimate that is above auditory curve estimated by FEM harmonic frequencies, but also constrained further by low frequency limit of 38 Hz, and high frequency limit of 1,243 Hz estimated from the tympanum and stapedial areas, according to scaling regression of these traits to hearing frequencies (41).

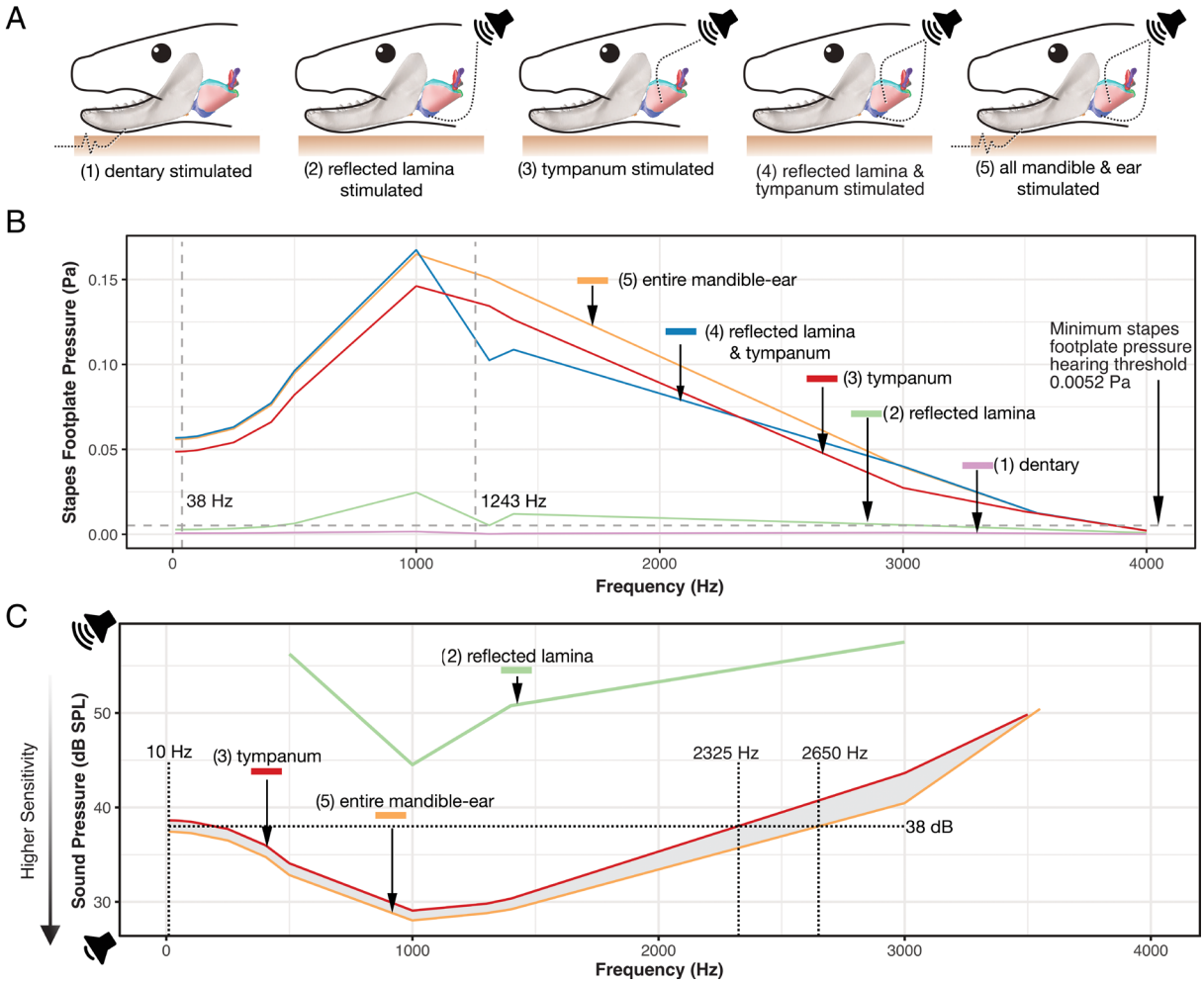

Fig. 4. Hearing sensitivity of the mandibular middle ear of *Thrinaxodon*. (*A*) Frequency response of constituent parts of the middle ear to simulated sound pressure: on dentary (A1), on ectotympanic reflected lamina (A2), on tympanum alone (A3), on both tympanum and ectotympanic (A4); and on the entire mandibular ear bones and tympanum (A5). (*B*) Harmonic response of mandibular middle ear, both as an integrated system, and by its individual components (including tympanum), as calibrated by the stapes footplate pressure (Y-axis in Pa) over hearing range (X-axis, in Hz). (*C*) Auditory area of *Thrinaxodon* mandibular ear and its components, estimated by FEM harmonic response (same as Fig. 3*B*). The gray area indicates that the estimate of the response of the entire mandibular ear is slightly better than by tympanum alone.

Anatomical Model Construction. The *Thrinaxodon* model was constructed by digitally segmenting the mandible and middle ear bones from μCT scans in Avizo v9, including the dentary, splenial, coronoid, angular, prearticular, surangular, articular, quadrate, quadratojugal, stapes, and fenestra vestibuli. Each segmentation was subsequently converted into a 3D surface mesh and imported into Geomagic v17 to smooth and repair holes in their triangulated surfaces. Retrodeformation was not necessary for the well-preserved specimen UCMP V40466, which exhibits no deformation (Movie S2). However, the malleus was missing the retroarticular process in specimen UCMP V40466. To repair this defect, the retroarticular process of specimen BP/1/7199 was grafted onto the articular of specimen UCMP V40466. Further, the ectotympanic has an uneven (likely incomplete) ventral edge of its reflected lamina, in both specimens UCMP V40466 and BPI/7/7199. This uneven edge of the reflected lamina was minimally restored in our 3D model (Movie S2: 00:21–00:24). We preferred the minimal reconstruction from the available fossil data. The same general process was used to build the FE model of mandible, middle ear, and fenestra vestibuli from the *Didelphis virginiana* (UCRC RV183) μCT scan.

The models were then imported into Strand7 for finite element modeling and meshed with four-noded tetrahedral elements. The tympanic membrane was reconstructed in Strand7 by inserting plate elements spanning the ectotympanic cleft ("angular fossa") (11). These plates were exported from Strand7, and back into Geomagic v17 for mesh cleaning, and then imported back into Strand7 for finite element modeling. Material properties of solid bones and the tympanic membrane (*SI Appendix*, Table S3) were derived from Koike et al. (53) and Lautenschlager et al. (54), respectively. Based on our survey of the material and structural properties of the tympana in extant mammals and other tetrapods (*SI Appendix*, Table S4), we conducted sensitivity analyses to account for the stiffness, thickness, and density of the tympanum in a range of these variables (*SI Appendix*, Text S4 and Fig. S6). Soft tissue connections of sutural ligaments and cartilaginous contacts between bones were modeled as beam elements. Sutures were built between all bones except the quadrato-articular (jaw) joint, which was modeled as cartilage. An annular ligament was constructed with beam elements to unite the stapes footplate with the fenestra vestibuli.

FEA Loading Conditions. The FE model of the mandibular ear of *Thrinaxodon* was used to perform an analysis of auditory response, including stapedial footplate pressure, across a hearing frequency range (bandwidth) (Figs. 3 and 4). Strand7 was used to assign boundary conditions and solve the FE analyses. Modal and harmonic response analyses were performed with the Natural Frequency Solver and Harmonic Response Solver, respectively. For all simulation models, a single node on both the medial and ventral surfaces of the mandibular symphysis was constrained against all rotations and translations to hold the model in place. To hold the dentary rigid, a constraint against all translations and rotations was placed on the canine as well as the 2nd, 4th, and 6th postcanines. These constraints were necessary to ensure mass participation in harmonic response was in the postdentary ear bones. These constraints mean that our FEM simulated hearing of the animal with its jaws closed, with the lower and upper teeth in contact. A node on the coronoid was constrained against medial translation to mimic the

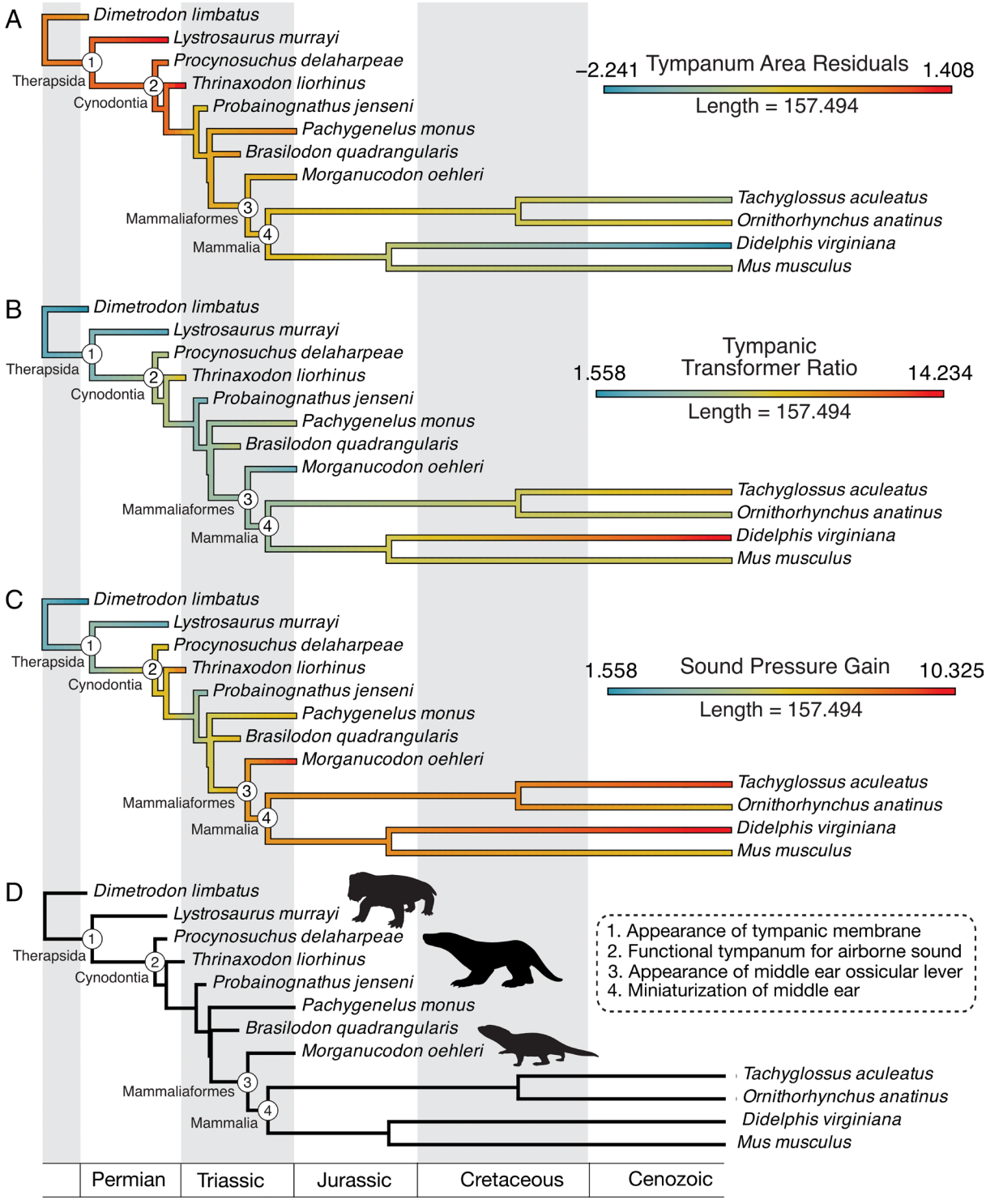

Fig. 5. Evolution of auditory capacity in synapsids-mammals by phylogenetic comparative methods for ancestral state reconstruction. (*A*) Evolution of hypothetical tympanum size across synapsids. (*B*) Evolution of the tympanic transformer ratio across synapsids. (*C*) Evolution of estimated sound pressure gain in the middle ear across synapsids. (*D*) Hypothesized stepwise evolution of auditory function in synapsids. The tympanic membrane first appeared in Therapsida (Node 1), a fully functioning soft-tissue tympanum reliant on airborne hearing and an effective transformer ratio evolved in Cynodontia (Node 2). The first appearance of an elaborated ossicular lever system in Mammaliaformes (Node 3). This further increased the ability of the middle ear to amplify sound at a wider hearing range occurred with the detached middle ear of crown Mammalia (Node 4).

pterygoid buttress. The postdentary ear bones were constrained according to the anatomical interpretation of Luo and Crompton (55). A single constraint against all translations and rotations was placed on the dorsal surface of the quadratojugal to maintain its rigid contact with the basicranium (not modeled here). A single constraint allowing only for ventral translation was placed on the dorsal surface of the quadrate, because the cranium would prevent dorsal translation (55). Constraints against all rotations and translations were placed on all sides of the fenestra vestibuli to immobilize the fenestra. The nodes on the caudal edge of tympanic membrane, where the tympanum spans the articular and the reflected lamina of the angular, were given the stiffness of skin (*SI Appendix*, Table S2) to mimic the thick skin which likely would have spanned the gap, as seen in opossums (15), monotremes (56, 57), and lizards (58). Other soft tissue structures, such as muscles, major ligamentous structures, and hyoid–jaw connections, were likely present (8, 15, 32) and could affect auditory sensitivity. However, anatomical

reconstruction of these soft- and hard-tissue structures is beyond the scope of our study. To model the effects of jaw adductor musculature activity on hearing capacity, we created three different model treatments where 1) a constraint against all translations and rotations was placed on the coronoid process, simulating active jaw adductor muscles); 2) nodes on the coronoid process were given the stiffness of flaccid muscle, simulating inactive but anatomically present jaw muscles; and 3) no constraints or stiffness were applied to the coronoid, simulating a hypothetical absence of jaw muscles (*SI Appendix*, Text S3 and Fig. S5).

A harmonic response analysis can be performed by two primary methods: the full harmonic method and the mode superposition method. The latter method computes the structural response by summing scaled mode shapes obtained from a preceding modal analysis. We adopted the mode superposition method because of its lower computational cost and significantly faster solution times than the full harmonic method. After application of boundary conditions, the Natural Frequency Solver, which is an analytic module in Strand7, was used to find 300 eigenmodes from 0 to 20,000 Hz. The results of the Natural Frequency Solver (i.e., calculation of mode shapes and their corresponding frequencies) are the input data for our harmonic response analysis. The Harmonic Response Solver was used to measure the response of the mandibular ear model to a harmonic load of 0.016 Pa [equivalent to 58.089 dB sound pressure level (SPL)] from 10 to 4,000 Hz, which is a hypothetical hearing range at which the stapedial footplate pressure decreases to 0 Pa. The input sound pressure is 30 dB above a best threshold at 28.089 dB as estimated by Phylogenetic Comparative Methods from a comparative dataset of best hearing thresholds of amphibians, reptiles, and mammals (Fig. 3 and *SI Appendix*, Table S1). To compare the frequency response of these different routes, or their combination(s), and to test their relative efficacy for hearing, we ran harmonic response analyses separately (Fig. 4): 1) on the soft-tissue tympanum (an evolutionarily derived structure) (Fig. 4, *A*3), 2) on the ectotympanic alone, in light of the hypothetical function of its reflected lamina in therapsids and cynodonts (Fig. 4, *A*4) (8, 44, 45), 3) on the dentary alone in light of its hypothetical function in contact hearing (Fig. 4, *A*1); 4) on the ectotympanic and tympanum together; and 5) on the whole mandible, including the tympanum (Fig. 4, *A*5) (21, 42).

FEA Result Assessment. Our methods are aimed at determining the sensitivity (in SPL) over the hearing range (in frequencies) of the auditory capability of *Thrinaxodon* from FEA Harmonic Response Analysis of the whole mandibular system. Our FEA model of mandibular ear system is also cross-verified against independent functional estimates from individual ear structuresof *Thrinaxodon* (Fig. 3*B*).

Independent estimates of auditory function. Three auditory parameters are fundamental for assessment of hearing performance of tetrapods in general, and for *Thrinaxodon* (and *Didelphis*): the lower frequency limit, higher frequency limit, and the best frequency that corresponds to the lowest SPL, also known as the best sensitivity threshold. Of these, the lower frequency limit and higher frequency limit can be independently estimated by a correlation of these parameters with tympanum size (area) and stapedial footplate size (area), on the basis of the power functions that relate the tympanum area and stapedial footplate area to these auditory parameters (21, 42) (*SI Appendix*, Table S1). See *SI Appendix*, Text S5 for discussion of the use of cochlea morphometrics to estimate auditory parameters (59).

Tympanum size. The area of the tympanum (soft-tissue tympanic membrane) was measured on the composite model of specimens UCMP V40466 and BP/1/7199 (Fig. 2 and *SI Appendix*, Table S1 and Movie S2), following the interpretation by Allin (8). Tympanum areas of other synapsids and mammals were taken from the literature (*SI Appendix*, Table S3). Scaling regression of tympanum size with mandible length and evolutionary changes of tympanum area in synapsid evolution are presented in Fig. 5 and *SI Appendix*, Figs. S7 and S8.

Stapedial footplate. The footplate of the stapes fits to the fenestra vestibuli and forms the junction of the middle and inner ears. The stapedial footplate of *Thrinaxodon* was measured in specimen UCMP V40466. Estimates of the stapedial footplate in comparative taxa of synapsids were taken from the literature (*SI Appendix*, Table S3).

Transformer ratio (TR) of tympanum and stapes footplate. Sound transfer from the tympanum through the malleus–incus–stapes to the inner ear was estimated by using the ratio of tympanum and stapedial footplate areas (21, 42, 60). This transformer ratio is an anatomical proxy of the pressure gain between the tympanum and the fenestra vestibuli, and of the impedance match of the air and the inner ear fluid. This metric was used for estimating the hearing frequency ranges and sensitivities (Fig. 2 and *SI Appendix*, Fig. S9).

$$TR = \frac{\frac{2}{3}A_{Tympanum}}{A_{Footplate}}, \quad [1]$$

where $A_{Tympanum}$ is the tympanum area (mm^2), $A_{Footplate}$ is the area of stapedial footplate (mm^2), and 2/3 is the ratio of the effective area for hearing function to the total area of tympanum (21, 42, 43).

Best sensitivity threshold. This threshold is defined by the lowest audible dB SPL. For auditory function of extant tetrapods, the best threshold is established by in vivo observation, but this threshold cannot be estimated from the bony anatomy of fossils. Here, we performed an ancestral state reconstruction by Phylogenetic Comparative Methods to estimate the best threshold for *Thrinaxodon*, using a comparative dataset of best hearing thresholds of amphibians, reptiles, and mammals (Fig. 3*A* and *SI Appendix*, Table S1). This estimate was performed using the R package ape (61) (https://CRAN.R-project.org/package=ape) with a synapsid–mammal phylogeny from Hellert et al. (13). We performed phylogenetic independent contrasts (pic), maximum likelihood (ML), and restricted maximum likelihood (REML) ancestral state reconstructions of the best threshold (Fig. 3*A* and *SI Appendix*, Fig. S1). Our estimate for the best threshold is 28.089 dB (Table 1).

To facilitate our FEA functional analysis of stapedial footplate pressure in Pascals (Pa) (Fig. 4*B*), this decibel threshold was then converted to Pa using Eq. **2** (62):

$$p = 2e^{-6} \cdot 10^{\left(\frac{L_p}{20}\right)}, \quad [2]$$

where p is the pressure in Pa (as measured by FEA) and L_p is the pressure (in dB).

FEA Estimates of Hearing Ranges and Pressure Gain. The next step in evaluating the efficacy of hearing function was to calibrate the minimal stapedial footplate pressure cutoff, above which *Thrinaxodon* would hear. This cutoff was defined by first calculating the frequency-dependent sound pressure gain of the system with Eq. **2**:

$$Gain = \frac{P_{output}}{P_{input}}, \quad [3]$$

where P_{input} is the input sound pressure applied to a given component of the mandibular ear (in our loading conditions 0.016 Pa/58.089 dB), and P_{output} is the output sound pressure at the stapedial footplate (Figs. 3*B* and 4*C*) to be computed by FEA. We then used the pressure gain and our estimated best threshold to calculate a minimal stapedial footplate pressure cutoff for hearing, using Eq. **4**:

$$P_{StapesMin} = Gain_{max} \cdot P_{BestThreshold}, \quad [4]$$

where $P_{StapesMin}$ is the minimal stapedial footplate pressure required to distort the cochlear duct to perceive sound, $Gain_{max}$ is the calculated gain at the best frequency (the frequency corresponding to best (lowest) sound pressure threshold), and $P_{BestThreshold}$ is the best (lowest) SPL. This Eq. (**4**) allowed us to compare our FEA results against independent estimates from other structures in the auditory system.

We measured stapes footplate pressure starting at 10 Hz until the results no longer met the stapedial footplate pressure cutoff (0.0052 Pa). Routes of sound conduction were considered "to be viable" if the stapes footplate pressure met or exceeded the cutoff pressure in the estimated *Thrinaxodon* hearing range (38.05 to 1,243 Hz) (Fig. 3*B*). We loaded our *Didelphis* model with sound pressures from an audiogram by an in vivo experimental study of *Didelphis* across its full hearing range (63). We then collected stapes footplate pressure under these conditions. To validate our assumptions, we checked that stapes footplate pressure was greater than or equal to an estimated minimal stapedial footplate pressure cutoff derived from best threshold (Eq. **4**), analogous to our *Thrinaxodon* FEM simulation. *Didelphis* results are presented in *SI Appendix*, Fig. S3.

We summarize the hearing range of *Thrinaxodon* in a conceptual audiogram (Fig. 4*C*) using the calculated gain from the FEA with Eq. **5**:

$$P_{Input} = \frac{P_{StapesMin}}{Gain_f}, \quad [5]$$

Table 1. Auditory parameter estimates from FEA harmonic response analyses, from phylogenetic comparative methods on best (lowest) hearing threshold, and from the tympanum and stapedial footplates.

Estimators of parameter	Lowest frequency	Best frequency	Highest frequency	Method reference
FE harmonic response at 38 dB and Tympanum area (mm^2)	38 Hz	890 Hz	1,243 Hz	Current Study and Rosowski and Graybeal (42)
FE harmonic response 38 dB and Stapes footplate area (mm^2)	38 Hz	741 Hz	1,243 Hz	Current Study and Rosowski and Graybeal (42)
FE harmonic response at 38 dB	10 Hz	1,000 Hz	2,325 Hz	Current study (tympanum estimate)
FE harmonic response at 38 dB	10 Hz	1,000 Hz	2,650 Hz	Current study (mandibular ear estimate)
	Best (Lowest) Threshold			
Phylogenetic comparative methods	28.09 dB			Current study & Data in *SI Appendix*, Table S1
	Minimal stapedial pressure			
FE harmonic response	0.0052 Pa			Eq. (**3**)

where P_{Input} is the input SPL (vertical axis of an audiogram) and $Gain_f$ is the pressure gain at a given frequency. For testing sound conduction routes, a route is considered to be functional across the estimated hearing range if the stapedial footplate pressure is greater than or equal to the stapedial footplate pressure cutoff. For the test case of *Didelphis,* our FEA simulation computed the stapedial footplate pressure reasonably accurately from 10 to 2,650 Hz at stapedial pressure of 0.0052 Pa (*SI Appendix*, Fig. S3 and Text S5). However, at higher frequencies (≥2,650 Hz), our FEA simulation deviated from the in vivo data (49) (*SI Appendix*, Fig. S3). This is likely because the static pressure at the stapes did not account for dynamic material properties of the cochlear duct, which is known to deform at higher frequencies under less pressure (49). Our model could be less sensitive to higher frequencies, for this reason (49), among other modeling factors (2). Despite these limitations, calculating the footplate pressure from FEA can help to rank the effectiveness of individual routes of hearing (Fig. 4).

Mapping of Hearing Function Across Synapsid Evolution. To evaluate phylogenetic evolution of the hearing function estimated by our FE analyses, we performed ancestral state reconstructions of biomechanically significant anatomical characters for hearing in synapsids (*SI Appendix*, Table S3), specifically the relative tympanum area, primary tympanic transformer ratio, and estimated maximum tympanic pressure gain.

We estimated the area of the tympanum and the area of the stapes footplate of synapsids from published graphics and images from the literature (*SI Appendix*, Table S3). The location of the tympanic membrane was reconstructed in the angular cleft following Allin (8). The angular cleft is an osteological proxy for tympanum size and was used for the analysis of the morphological transformations of the tympanum. As a size-correcting step, we calculated residuals from the linear regression of log-transformed tympanic membrane area on log-transformed jaw length (*SI Appendix*, Fig. S4), which were then mapped on a synapsid phylogeny. Sound transfer from the tympanum through the malleus–incus–stapes to the inner ear was also estimated by using the ratio of tympanum area and stapedial footplate area, also known as the primary tympanic transformer or area ratio (21, 42). The primary tympanic transformer ratio was calculated with Eq. **1**.

The estimates of maximum tympanic gain are mostly based on the primary tympanic transformer ratio in synapsids through stem mammaliaforms (Fig. 5, Node 3). In crown Mammalia, the incus (long process) and malleus (manubrium) are a fully developed lever system, which made it feasible for us to calculate maximum gain from both the mechanical advantage of the middle ear levers and the primary tympanic transformer ratio (Fig. 5, Node 4).

Allometrically corrected tympanum size, primary tympanic transformer ratio, and estimated tympanic maximum gain were mapped on to a synapsid phylogeny with ancestral state reconstruction in the R package ape, using the pic, ML, and REML methods. The results with the narrowest 95% CI ranges are reported in Fig. 5 and more details are given in Fig. 5 and *SI Appendix*, Fig. S8.

Results

Analysis of Auditory Parameters. Lower frequency hearing limit, best frequency, upper hearing frequency limit, and best threshold were predicted from multiple estimators of the middle ear (Fig. 3 and Table 1 and *SI Appendix*, Table S2). The metrics with the best statistical support were used to determine frequencies and volumes at which *Thrinaxodon* could likely register sound (Fig. 3). These parameters allowed us to evaluate whether the FEM produces enough stapedial footplate pressure for *Thrinaxodon* to register sound within an audible frequency range that was independently estimated for *Thrinaxodon*.

Ancestral state reconstructions were used to generate a best threshold estimate for *Thrinaxodon*. All three ancestral state reconstruction methods produced similar results for the amniote node, which are close to the average tetrapod best threshold (Fig. 3*A*). Thus, we set best threshold at 28.089 dB.

Allometrical power functions of two traits (tympanum area and stapedial plate area) were used as additional, independent estimates of the hearing frequency range of *Thrinaxodon*. The lowest frequency was determined to be 38.05 Hz, and the highest frequency was determined to be 1,243 Hz (Fig. 3*B*). The best hearing frequency was estimated to be about 741 Hz based on stapedial footplate area, or about 890 Hz based on tympanum area (Table 1).

From FEA and our stapedial footplate pressure hearing cutoff criterion, we obtained a broader estimated hearing range, with a low limit of 10 Hz and a high limit of 2,325 Hz (when only the tympanum was stimulated) to 2,650 (when the entire mandibular middle ear was stimulated), at 38 dB SPL. This was an arbitrary SPL used to create a parabolic pseudoaudiogram, without further constraints by functional characters of tympanum area and stapedial footplate area (Figs. 3*B* and 4*C*). The greatest sensitivity of hearing occurred around 1,000 Hz (Fig. 3*B* and Table 1).

Comparison of Sound Conduction Routes. There are several sound-conducting routes in the mandibular middle ear. A sinusoidal sound pressure was applied to the different parts of the mandibular middle ear (Fig. 4*A*): 1) the ventral dentary, 2) the reflected lamina, 3) the tympanum, 4) the reflected lamina and the tympanum, and 5) the entire mandible and ear. All of these routes were tested with the same auditory parameters postulated for *Thrinaxodon* (frequency range of 38 to 1,243 Hz at 38 dB SPL; minimal best threshold at 28 dB and stapedial pressure at 0.0052 Pa) (Fig. 3) (20, 40). Each of these routes was considered

functioning if the stapes footplate registered its minimal pressure of 0.0052 Pa or more.

Our most important result is that sound pressure on the tympanum alone yielded sufficient pressure (≥0.0052 Pa) at the stapedial footplate for hearing across the estimated frequency range (Fig. 3 *A* and *B*). By comparison, sound pressure (either substrate-borne, or airborne) exclusively on the reflected lamina only generated enough pressure at the stapedial footplate for hearing near 1,000 Hz (Fig. 3 *A* and *B*). Footplate pressure associated with substrate-borne sound (modeling jaw–ground contact) did not produce enough stapedial pressure to meet the minimal stapedial footplate pressure cutoff (Fig. 3 *A* and *B*). Sound stimulation on the combined tympanum and bones (ectotympanic and dentary) slightly improved the hearing sensitivity (Fig. 4*B*).

An additional consideration of our *Thrinaxodon* model is its sensitive response to the dual musculoskeletal functions of the mandible for feeding and hearing. Since the mandibular ear is an integral part of the jaw hinge, hearing function and jaw muscle action for feeding should interact with each other. Our *Thrinaxodon* model also considered the potential impact of chewing action on sound perception (*SI Appendix*, Text 3). Isometric contraction of the temporalis muscles had frequency-dependent impacts on auditory sensitivity (*SI Appendix*, Fig. S5). At lower (10 to 1,000 Hz) frequencies, a simulated active temporalis muscle slightly increased the model sensitivity for auditory response (*SI Appendix*, Fig. S5*B*). Over the hearing frequency range of 1 to 2,500 Hz, the model with inactive (relaxed) temporalis muscles, had a better sensitivity at a lower auditory threshold (*SI Appendix*, Fig. S5*C*). At 2,500 Hz, activating the temporalis muscle increased auditory sensitivity and extended the hearing range (*SI Appendix*, Fig. S5*D*). Our *Thrinaxodon* model illustrates how jaw muscles and feeding may influence the function of hearing in a mandibular middle ear.

We observed that sound stimulation on combined mandibular bones and the tympanum can improve auditory function for *Thrinaxodon* relative to stimulation of the tympanum alone (Fig. 4*C*). We further note that the profile of the harmonic response curve of the entire mandibular middle ear is comparable between stimulation on the integrated ectotympanic-tympanum and the stimulation on the tympanum only. If the ectotympanic (including its prominent plate-like structure) is stimulated, the hearing sensitivity is significantly lower than tympanum alone (Fig. 4*C*). Sound pressure on the dentary (either substrate-borne or airborne sound) without the tympanum did not meet the minimal hearing threshold over the estimated range of frequencies.

Phylogenetic Analyses. Ancestral state reconstruction gives unique insight into the origin of a functional tympanum in synapsid-mammal evolution (Fig. 5 and *SI Appendix*, Figs. S8–S10). Using residuals of tympanum area (*SI Appendix*, Fig. S6), we found a trend of increasing relative tympanum size, beginning with the ancestor of Therapsida (Fig. 5*A*, Node 1), and then another trend to miniaturization of the tympanum (Fig. 5*A*), consistent with the overall reduction of body mass in the cynodont–mammaliaform transition (12, 52). Early synapsids and most therapsids (11) did not have a large enough tympanic membrane relative to the stapedial footplate (tympanic transformer ratio) to detect airborne sound with harmonic pressure applied to the tympanum alone (Fig. 5*B*). An increase in the tympanic transformer ratio came with cynodonts, later in evolution, accompanied by increases in tympanum vs. stapes pressure gain (Fig. 5*A*). A narrow soft-tissue tympanic membrane was likely present already in therapsids (8, 11, 12, 45), but it is not until cynodonts that the tympanum was large enough to become a functional sound receiver, as indicated by the new data on the tympanum transformer ratio and stapedial pressure gain (Fig. 5 *A* and *B*).

Discussion

These analyses and data are comprehensive biomechanical assessment of the earliest-known functional tympanic membrane in a nonmammalian therapsid, as exemplified by *Thrinaxodon* (Fig. 1). Our most important finding is that our data support the hypothesis that the soft-tissue tympanum is the most effective route for hearing in *Thrinaxodon*. Sound pressure at the tympanum alone could generate stapedial footplate pressure above our estimated hearing cutoff of 0.0052 Pa across the estimated hearing range. This demonstrates that the reconstructed tympanum in *Thrinaxodon* (Figs. 2 and 4) is sufficient for hearing by this extinct cynodont. Our results suggest a surprisingly "mammal-like" mode of hearing in this stemward taxon, despite its possession of a mandibular middle ear. With a neomorphic soft-tissue tympanum as the main receiver for sound, our data provide evidence that *Thrinaxodon* had already transitioned to reliance on direct hearing of airborne sound. Our FEA also shows that conduction routes through the mandible had a complementary (although limited) contribution to the overall hearing function of *Thrinaxodon*.

The material properties of the soft tissue tympanum make it more effective at detecting a broader range of frequencies (especially higher frequencies) and more sensitive to lower SPLs. This contrasts with sound transmitted through bone conduction, or directly via the skull to the ear bones. Mass participation in the harmonic response by bony elements will decrease at higher frequencies because of the damping properties of bone (53). This means that mandibular ear bones, by themselves, are likely limited to sound reception at lower frequencies (53) (*SI Appendix*, Fig. S2). The functional innovation is in the soft-tissue tympanum—the neomorphic part of the mandibular ear—which enables *Thrinaxodon* to expand its hearing to a more mammal-like range of frequency sensitivity (Figs. 1 and 3). Without the tympanum and the bony reflected lamina, the dentary alone could not generate enough pressure at the stapedial footplate to meet our estimated hearing threshold across all frequencies (Fig. 4*B*). Likewise, the reflected lamina of the ectotympanic bone, by itself, could generate only a very low level of stapedial footplate pressure across the full frequency range (Fig. 4*B* and *SI Appendix*, Fig. S4), which was well below the better sensitivity level of the tympanum.

Estimating auditory parameters for a nonmammalian cynodont by correlations and scaling analysis from extant sauropsids and mammals (42) can produce biased estimates. These estimates assume similar allometrical patterns of middle ear size for both extinct therapsids and extant mammals. But it is now demonstrated (45) that sound-receiving structures can show distinct allometrical patterns, specific to individual therapsid clades (see also Fig. 5*A*). Moreover, these analyses (unlike FEA) cannot account for the stiffness of the attachment between the middle ear and dentary in nonmammalian therapsids (42), which could limit middle ear motion or perhaps even increase hearing sensitivity at higher frequencies (*SI Appendix*, Fig. S5; 42, 53) beyond what would be expected from studying the bony middle ear in isolation. Despite these technical limits on estimation of auditory parameters by regression analysis, we believe these estimates represent an independent test of the auditory function inferred from FEA of the middle ear (Fig. 3). As such, it still is currently the best test for the hypothetical hearing ranges of *Thrinaxodon*.

Our harmonic response analyses on the constituent structures of the mandibular-ear system of *Thrinaxodon* are comprehensive in

covering all functional scenarios proposed previously and yields a key insight: The soft-tissue tympanum is the main structure that expands auditory function for a wider hearing range to higher frequencies at better sensitivity. We performed a series of ad hoc sensitivity analyses on the material property parameters of the tympanum (*SI Appendix*, Text S4) over a range of values reported in the literature (*SI Appendix*, Table S4). We found that soft tissue tympana of differing properties generate similar model results within this range of variable parameter values (*SI Appendix*, Fig. S6).

The air chamber (recessus mandibularis) internal to the ectotympanic cleft in therapsids provided a useful resonance chamber (Fig. 5*A*) (11). The homologous mandibular air chamber and the ectotympanic cleft are further enlarged in cynodonts (8, 11, 43). The larger air chamber and soft-tissue tympanum are key for *Thrinaxodon* to develop a much more mammal-like hearing relative to precynodont therapsids (Figs. 1 and 3), representing a major phylogenetic transition (Fig. 5: crownward from node 2).

The ectotympanic reflected lamina of therapsids shows surface features that suggest that it served a sound reception function (8, 11, 34, 36, 43–45, 53) (Fig. 1*A*). The ectotympanic reflected lamina could also transfer sound to the tympanum suspended from it, analogous to the bone conduction from the hyoid to ectotympanic in bats (51). Our functional estimate on the reflected lamina of *Thrinaxodon* indicates that a harmonic load on this structure alone can result in stapedial footplate pressure of 0.0052 Pa over a hearing range from 10 to 2,600 Hz (Fig. 4*B*), but at much less sensitivity than the tympanum. For the reflected lamina to approach the level of sound pressure gain of the tympanum (*SI Appendix*, Fig. S5), it would have to be five times larger than in this *Thrinaxodon* FEM. This observation is consistent with the earlier intuitive interpretation of the tympanum over the air-chamber of recessus mandibularis for *Thrinaxodon* by Allin (8) and corroborates the previous interpretation of a somewhat limited auditory capability of the ectotympanic reflected lamina (8, 11).

It is widely accepted that the larger tympanum of *Thrinaxodon* is an evolutionary novelty of cynodonts in its own right, relative to the anatomy of therocephalians. But our FEM provides concrete metrics of the capability of *Thrinaxodon* for direct airborne sound reception with a soft tympanum (Fig. 3*A*), just like extant mammals, with or without the aid of bone conduction from mandibular ear bones. Although our analysis clearly shows *Thrinaxodon* lacked a sufficient sensitivity to higher frequencies above 3,000 Hz, as previously suggested for cynodonts (64, 65), the functional mammal-like tympanum makes the ear much more sensitive than the ear would be from bone conduction of sound alone (Fig. 4). Despite being viewed as a transitional morphotype of cynodont ear evolution, the middle ear of *Thrinaxodon* likely relied on the tympanum in a remarkably mammal-like manner.

Using phylogenetic comparative methods, we can quantitatively estimate the functional evolution of the middle ear across synapsid phylogeny (Fig. 5). In precynodont synapsids, the tympanum was likely far too small to be a viable sound receiver (Fig. 5*A*, node 1). If a tympanum developed in the ancestor of Therapsida, its surface area would be an intermediate, between the plesiomorphic basal synapsids, many of which are atympanic, and a full eardrum of the Cynodontia (Fig. 5*A*, node 2). Further development of an elaborated ossicular lever system in mammaliaforms, including a neomorphic stapedial process of the incus (3, 21, 43), further increased the tympanic transformer ratio for sound transmission, potentially compensating for decreasing tympanum size in mammaliaforms (Fig. 5, node 3) (54). In crown mammals (Fig. 5, node 4), detachment of the middle ear from the jaw resulted in different evolutionary trajectories for morphofunctional traits in the jaw and middle ear (66). It is important to note, however, that these transformations do not represent a scala naturae toward mammal-like traits; rather, these are adaptive peaks specific to different auditory functional demands (44), such as locating prey, avoiding predators, parental care, or mating. Thus, it is not unexpected that the estimated increase in hearing capability does not show a simple linear evolutionary change across synapsids. Notably, tympanic hearing offers dramatically better auditory sensitivity (lowered threshold for more sensitive hearing) (Fig. 4). Thus, we hypothesize that requirements for hearing softer sounds drove the transition to tympanic hearing (Fig. 5, node 2).

Our preferred hypothesis is that cynodonts had transitioned to the tympanic membrane as a primary receiver reliant on airborne sound, in contrast to a mandibular ear system in precynodont synapsids, which lacked such a tympanum (Fig. 5). The hypothesized bone conduction hearing of substrate-borne lower frequency sound through the mandible is ancestral to synapsids, because most of the earlier synapsids are atympanic and lack an angular (ectotympanic) cleft (Fig. 5). This is consistent with the ancestral atympanic condition of diapsids, many of which can hear well as discussed previously (2, 11, 21, 43–45, 64, 65, 67, 68).

A full tympanum capable of direct sound reception, on top of sound stimulation via reflected lamina, is a novelty of *Thrinaxodon* (Fig. 4*A*), as demonstrated here. The hypothesized transition from reliance on bone-conducted sound to reliance on tympanic hearing likely occurred much earlier in therapsid evolution than previously understood (3).

Conclusions

The middle ear with tympanum, malleus, and incus detached from the mandible, is a defining trait of living mammals and is associated with more sensitive hearing (5, 24, 41). Here, we offer a hypothesis regarding the evolution of the soft-tissue tympanum based on a biomechanical model of the mandibular middle ear of *Thrinaxodon*, which occupies a transitional position in therapsid-mammal evolution. We estimated auditory function using harmonic response analysis of the middle ear, independently constrained by parameters estimated by phylogenetic comparative modeling (Figs. 1, 3, and 5).

Our harmonic response analysis supports the hypothesis that the tympanic membrane in *Thrinaxodon* is the primary sound receiver, and that a conservative estimate of hearing range of *Thrinaxodon* is from 38 to 1,243 Hz, with highest sensitivity at 1,000 Hz at an incident sound pressure of 28 dB (estimated by FEM harmonic response) or 740 Hz (FEM plus the estimate from stapedial footplate area). From the new data and analyses, we further argue that bone conduction through the mandible would have slightly improved hearing in *Thrinaxodon* but was much less important than the neomorphic tympanum in driving hearing performance. This clarifies the relative importance of the bone conduction vs. direct reception of airborne sound and their respective routes in the structural components of the mandible-attached ear of cynodonts, beyond what could be resolved by previous qualitative studies. Phylogenetic analysis shows that any precynodont therapsid mandibular ear still did not have a sufficiently functional tympanum. Tympanic hearing became effective only in cynodonts. These results provide the foundation for future investigations into the evolution of synapsid hearing.

Data, Materials, and Software Availability. Study data are included in the article and/or supporting information.

ACKNOWLEDGMENTS. We thank Dr. Patricia Holroyd (University of California Museum of Paleontology) for providing the *Thrinaxodon* specimens for this study, and for access to fossil collection. We are indebted to John Peacock, Kaleb Sellers, Casey Holliday, Ken Angielczyk, and Christian Kammerer for insightful feedback and discussion. We thank April I. Neander for help with CT scanning and with graphics and movies of this work. This work was funded by the University of Chicago Department of Organismal Biology and Anatomy, training fellowship to A.T.W. from NINDS NIH T32NS121763-01A1, and funding to C.F.R. and Z.-X.L. from NSF (IOS 2315501). This manuscript was significantly improved by feedback from two anonymous reviewers.

Author affiliations: [a]Department of Organismal Biology and Anatomy, The University of Chicago, Chicago, IL 60637

1. R. R. Fay, *Hearing in Vertebrates: A Psychophysics Databook* (Hill-Fay Associates, 1988).
2. J. Christensen-Dalsgaard, G. A. Manley, "The malleable middle ear: an underappreciated player in the evolution of hearing in vertebrates" in *Insights from Comparative Hearing Research, Springer Handbook of Auditory Research*, C. Köppl *et al.*, Eds. (Springer, 2013), vol. 49, pp.157–191. DOI 10.1007/2506_2013_33.
3. Z.-X. Luo, G. A. Manley, "Origins and evolution of mammalian ears and hearing function" in *The Senses–A Comprehensive Reference*, B. Fritzsch, B. Grothe, Eds. (Elsevier Academic Press, ed. 2, 2020), vol. 2, pp. 207–252, https://doi.org/10.1016/B978-0-12-805408-6.00033-6.
4. Z. Kielan-Jaworowska, R. L. Cifelli, Z.-X. Luo, *Mammals from the Age of Dinosaurs: Origins, Evolution, and Structure* (Columbia Univ. Press, 2004).
5. Z.-X. Luo, Transformation and diversification in the early mammalian evolution. *Nature* **450**, 1011–1019 (2007).
6. M. A. O'Leary *et al.*, The placental mammal ancestor and the post–K-pg radiation of placentals. *Science* **339**, 662–667 (2013).
7. T. A. Vaughan, J. M. Ryan, N. J. Czaplewski, *Mammalogy* (Jones and Bartlett Learning, ed. 6, 2013).
8. E. F. Allin, Evolution of the mammalian middle ear. *J. Morph.* **147**, 403–437 (1975).
9. T. S. Kemp, *The Origin and Evolution of Mammals* (Oxford University Press, 2005).
10. T. S. Kemp, "Non-mammalian synapsids: the beginning of the mammal line" in *Evolution of the Vertebrate Ear: Evidence from the Fossil Record, Springer Handbooks for Auditory Research*, J. A. Clack, R. R. Fay, A. N. Popper, Eds. (Springer, 2016), vol, 59, pp. 107–138.
11. S. L. Olroyd, C. A. Sidor, Nomenclature, comparative anatomy, and evolution of the reflected lamina of the angular in non-mammalian synapsids. *J. Vertebr. Paleontol.* **42**, e2101923 (2022).
12. C. A. Sidor, Evolutionary trends and the origin of the mammalian lower jaw. *Paleobiology* **29**, 605–640 (2003).
13. S. M. Hellert *et al.*, Derived faunivores are the forerunners of major synapsid radiations. *Nat. Ecol. Evol.* **7**, 1903–1913 (2023).
14. T. Kitazawa *et al.*, Developmental genetic bases behind the independent origin of the tympanic membrane in mammals and diapsids. *Nat. Commun.* **6**, 6853 (2015), 10.1038/ncomms7853.
15. D. J. Urban *et al.*, A new developmental mechanism for the separation of the mammalian middle ear ossicles from the jaw. *Proc. R. Soc. B Biol. Sci.* **284**, 20162416 (2017), 10.1098/rspb.2016.2416.
16. H.-D. Sues, The skull and dentition of two tritylodontid synapsids from the lower Jurassic of western North America. *Bull. Mus. Comp. Zool.* **151**, 217–268 (1986).
17. J. A. Hopson, J. W. Kitching, A probainognathian cynodont from South Africa and the phylogeny of nonmammalian cynodonts. *Bull. Mus. Comp. Zool.* **156**, 5–35 (2001).
18. J. F. Bonaparte, A. G. Martinelli, C. L. Schultz, New information on *Brasilodon* and *Brasilitherium* (Cynodontia, Probainognathia) from the late Triassic of southern Brazil. *Rev. Bras. Paleontol.* **8**, 25–46 (2005).
19. J. R. G. Rawson *et al.*, Brazilian fossils reveal homoplasy in the oldest mammalian jaw joint. *Nature* **634**, 381–388 (2024).
20. K. A. Kermack *et al.*, The skull of *Morganucodon*. *Zool. J. Linn. Soc.* **71**, 1–158 (1981).
21. K. A. Kermack, F. Mussett, The ear in mammal-like reptiles and early mammals. *Acta Palaeontol. Pol.* **28**, 147–158 (1983).
22. A. W. Crompton, Z.-X. Luo, "Relationships of the Liassic mammals *Sinoconodon*, *Morganucodon*, and *Dinnetherium*" in *Mammal Phylogeny: Mesozoic Differentiation, Multituberculates, Monotremes, Early Therians, and Marsupials*, F. S. Szalay *et al.*, Eds. (Springer-Verlag, 1993), pp. 30–44.
23. Q. Ji *et al.*, A swimming mammaliaform from the Middle Jurassic and ecomorphological diversification of early mammals. *Science* **311**, 1123–1127 (2006).
24. Z.-X. Luo, Developmental patterns in Mesozoic evolution of mammal ears. *Ann. Rev. Ecol., Evol. Syst.* **42**, 355–380 (2011).
25. Q.-J. Meng *et al.*, An arboreal docodont from the Jurassic and mammaliaform ecological diversification. *Science* **347**, 764–768 (2015).
26. C.-F. Zhou *et al.*, New jurassic mammaliaform sheds light on early evolution of mammal-like hyoid bones. *Science* **365**, 276–279 (2019).
27. F.-Y. Mao *et al.*, Fossils document evolutionary changes of jaw joint to mammalian middle ear. *Nature* **628**, 576–581 (2024).
28. Z.-X. Luo *et al.*, A new eutriconodont mammal and evolutionary development of early mammals. *Nature* **446**, 288–293 (2007).
29. J. Meng *et al.*, Transitional mammalian middle ear from a new Cretaceous Jehol eutriconodont. *Nature* **472**, 181–185 (2011).
30. F.-Y. Mao *et al.*, Integrated hearing and chewing modules decoupled as shown in a new Cretaceous mammal. *Science* **367**, 305–308 (2020).
31. J. Wang *et al.*, A monotreme-like auditory apparatus in a Middle Jurassic haramiyidan. *Nature* **590**, 279–283 (2021).
32. N. Anthwal *et al.*, Meckel's cartilage breakdown offers clues to mammalian middle ear evolution. *Nat. Ecol. Evol.* **1**, 0093 (2017).
33. T. S. Westoll, The mammalian middle ear. *Nature* **155**, 114–115 (1945).
34. D. M. S. Watson, The evolution of the mammalian ear. *Evolution* **7**, 159–177 (1953).
35. C. C. D. Shute, The evolution of the mammalian eardrum and tympanic cavity. *J. Anat.* **90**, 261–281 (1956).
36. J. A. Hopson, The origin of the mammalian middle ear. *Am. Zool.* **6**, 437–450 (1966).
37. E. F. Allin, "The auditory apparatus of advanced mammal-like reptiles and early mammals" in *The Ecology and Biology of Mammal-like Reptiles*, N. Hotton *et al.*, Eds. (Smithsonian Institution Press, 1986), pp. 283–294.
38. E. F. Allin, J. A. Hopson, "Evolution of the auditory system in Synapsida ("mammal-Like reptiles" and primitive mammals) as seen in the fossil record" in *The Evolutionary Biology of Hearing*, D. Webster *et al.*, Eds. (Springer, 1992), pp. 587–614.
39. A. W. Crompton, W. L. Hylander, "Changes in mandibular function following the acquisition of a dentary-squamosal joint" in *The Ecology and Biology of Mammal-like Reptiles*, N. Hotton *et al.*, Eds. (Smithsonian Institution Press, 1986), pp. 263–282.
40. A. Tumarkin, On the evolution of the auditory conducting apparatus: A new theory based on functional considerations. *Evolution* **9**, 221–243 (1955).
41. Z.-X. Luo, J. A. Schultz, E. G. Ekdale" Evolution of the middle and inner ears of mammaliaforms: The approach to mammals" in *Evolution of the Vertebrate Ear: Evidence from the Fossil Record, Springer Handbooks for Auditory Research*, J. A. Clack *et al.*, Eds. (Springer, 2016), vol. 59, pp. 139–174, DOI 10.1007/978-3-319-46661-3_6.
42. J. J. Rosowski, A. Graybeal, What did *Morganucodon* hear? *Zool. J. Linn. Soc.* **101**, 131–168 (1991).
43. T. S. Kemp, Acoustic transformer function of the postdentary bones and quadrate of a nonmammalian cynodont. *J. Vertebr. Paleont.* **27**, 431–441 (2007).
44. M. Laaß, The origins of the cochlear and impedance matching hearing in synapsids. *Acta Palaeontol. Pol.* **61**, 267–280 (2016), 10.4202/app.00140.2014.
45. S. L. Olroyd, B. T. Kopperud, Allometry of sound reception structures and evidence for a mandibular middle ear in non-mammalian synapsids. *Evolution* **79**, 905–921 (2025).
46. B. Szabó, I. Babuška, *Finite Element Analysis: Method, Verification and Validation* (Wiley, Hoboken, NJ, ed. 2, 2021), pp. 1–369.
47. R. Z. Gan, B. P. Reeves, X. Wang, Modeling of sound transmission from ear canal to cochlea. *Ann. Biomed. Eng.* **35**, 2180–2195 (2007).
48. R. Claes *et al.*, Eardrum and columella displacement in single ossicle ears under quasi-static pressure variations. *Hear. Res.* **365**, 141–148 (2018).
49. H. Motallebzadeh, S. Puria, Stimulus-frequency otoacoustic emissions and middle-ear pressure gains in a finite-element mouse model. *J. Acoust. Soc. Am.* **152**, 2769–2780 (2021).
50. M. Ugarteburu *et al.*, Mammalian middle ear mechanics: A review. *Front. Bioeng. Biotechnol.* **10**, 983510 (2022), 10.3389/fbioe.2022.983510.
51. C. C. G. Snipes, R. T. Carter, Vibroacoustic response of the tympanic membrane to hyoid-borne sound generated in during echolocation in bats. *Integr. Org. Biol.* **5**, obad004 (2023).
52. V. Fernandez *et al.*, Synchrotron reveals Early Triassic odd couple: Injured amphibian and aestivating therapsid share burrow. *PLoS One* **8**, e64978 (2013).
53. T. Koike *et al.*, Modeling the human middle ear using the finite-element method. *J. Acoust. Soc. Am.* **111**, 1306–1317 (2002).
54. S. Lautenschlager *et al.*, The role of miniaturisation in the evolution of the mammalian jaw. *Nature.* **561**, 533–537 (2018), 10.1038/s41586-018-0521-4.
55. Z.-X. Luo, A. W. Crompton, Transformations of the quadrate (incus) through the transition from non-mammalian cynodonts to mammals. *J. Vertebr. Paleont.* **14**, 341–374 (1994).
56. L. M. Aitkins, B. M. Johnstone, Middle ear function in a monotreme: The echidna (*Tachyglossus aculeatus*). *J. Exp. Zool.* **180**, 245–250 (1972).
57. G. R. Gates *et al.*, Peripheral auditory function in the platypus, *Ornithorhynchus anatinus*. *J. Acoust. Soc. Am.* **56**, 152–156 (1974).
58. E. G. Wever, *The Reptile Ear* (Princeton University Press, 1978).
59. C. Köppl, G. A. Manley, A functional perspective on the evolution of the cochlea. *Cold Spring Harb. Perspect. Med.* **9**, 1–14 (2019), 10.1101/cshperspect.a033241.
60. E. G. Wever, M. Lawrence, *Physiological Acoustics* (Princeton University Press, 1954).
61. R-Team, R: A Language and Environment for Statistical Computing. http://www.R-project.org/ (R Foundation for Statistical Computing, 2013).
62. L. Laccourreye, O. Laccourreye, A century ago, the birth of the decibel. *Eur. Ann. Otorhinolaryngol. Head Neck Dis.* **141**, 305–307 (2024).
63. R. J. Ravizza *et al.*, Hearing in primitive mammals: I, Opossum (*Didelphis virginiana*). *J. Aud. Res.* **9**, 1–7 (1969).
64. M. Laaß, Bone conduction hearing and seismic sensitivity of the late Permian anomodont *Kawingasaurus fossilis*. *J. Morph.* **276**, 121–143 (2014).
65. G. A. Manley, Evolutionary paths to the mammal cochlea. *J. Assoc. Res. Otolaryngol.* **13**, 733–743 (2012).
66. Z. J. Tseng *et al.*, A switch in jaw form–function coupling during the evolution of mammals. *Phil. Trans. R. Soc. Lond. B Biol. Sci.* **378**, 20220091 (2023), 10.1098/rstb.2022.0091.
67. G. Capshaw, J. Christensen-Dalsgaard, C. E. Carr, Hearing without a tympanic ear. *J. Exp. Biol.* **225**, jeb244130 (2022).
68. M. Bronzati *et al.*, Deep-time origin of tympanic hearing in crown reptiles. *Curr. Biol.* **34**, 1–7 (2024).